NASA MEMO 1-16-59L

NASA

MEMORANDUM

SEMIEMPIRICAL PROCEDURE

FOR ESTIMATING LIFT AND DRAG CHARACTERISTICS OF

PROPELLER-WING-FLAP CONFIGURATIONS FOR VERTICAL-

AND SHORT-TAKE-OFF-AND-LANDING AIRPLANES

By Richard E. Kuhn

Langley Research Center
Langley Field, Va.

NATIONAL AERONAUTICS AND
SPACE ADMINISTRATION

WASHINGTON

February 1959

NATIONAL AERONAUTICS AND SPACE ADMINISTRATION

MEMORANDUM 1-16-59L

SEMIEMPIRICAL PROCEDURE FOR ESTIMATING LIFT AND DRAG CHARACTERISTICS OF PROPELLER-WING-FLAP CONFIGURATIONS FOR VERTICAL- AND SHORT-TAKE-OFF-AND-LANDING AIRPLANES

By Richard E. Kuhn

SUMMARY

The analysis presented uses the momentum theory as a starting point in developing semiempirical expressions for calculating the effect of propeller thrust and slipstream on the lift and drag characteristics of wing-flap configurations that would be suitable for vertical-take-off-and-landing (VTOL) and short-take-off-and-landing (STOL) airplanes. The method uses power-off forward-speed information and measured slipstream deflection data at zero forward speed to provide a basis for estimating the lift and drag at combined forward speed and power-on conditions. A correlation of slipstream deflection data is also included. The procedure is applicable only in the unstalled flight regime; nevertheless, it should be useful in preliminary design estimates of the performance that may be expected of VTOL and STOL airplanes.

INTRODUCTION

There is currently a great deal of interest in various VTOL and STOL airplanes. The propeller-driven types, in particular, have been subject to numerous investigations. (See refs. 1 to 20.) At present, the estimation of the performance characteristics of these types in the transition speed range usually requires the use of wind-tunnel power-on lift and drag data. A simple procedure for estimating the lift and drag characteristics of propeller-wing-flap configurations that could be used in the preliminary design stage before wind-tunnel tests of a specific configuration are available would be helpful.

The present report attempts to provide such an estimating procedure in the unstalled flight regime. The analysis makes use of the momentum theory as a starting point in developing a semiempirical method for estimating the effects of propeller slipstreams at high-power conditions.

The method utilizes the large body of slipstream deflection data at zero forward speed or hovering, on the one hand, and conventional power-off wing-flap information, on the other hand, as a basis for the calculations. The method, in effect, provides a logical means of interpolating between these end points.

The procedure presented herein is applicable only in the unstalled region of flight; nevertheless, it should be of some use in estimating the best performance that can be obtained in the absence of stall. As in the conventional power-off case, the estimation of maximum lift and the characteristics beyond the stall involves the application of more art than science. Experience and wind-tunnel tests will be needed to tailor properly the wing-flap system to avoid or minimize the stall in any specific case. A discussion of the consequences of wing stall on the transition performance of propeller-driver VTOL and STOL airplanes and of ways of eliminating or reducing stalling is presented in reference 21.

COEFFICIENTS AND SYMBOLS

With a wing operating in the slipstream of a propeller, large forces and moments can be produced even at very small free-stream velocities. For this condition, the coefficients based on the free-stream dynamic pressure approach infinity as the free-stream velocity approaches zero and thus become less useful. It appears appropriate, therefore, to base the coefficients on the dynamic pressure in the propeller slipstream. This system has been used in reporting much of the recent experimental work on wing-propeller configurations. It is a useful and easily handled system when working with airplanes that are expected to hover. The values of the coefficients, however, are not familiar and, therefore, are not as meaningful to most people as conventional coefficients. For this reason, when dealing with configurations that are not expected to hover, the more commonly used coefficients, based on the free-stream velocity, would probably be preferred. Therefore, for convenience, in many instances in this report, equations and data are presented based on both systems. The conversion from one system to the other is very simple and is shown at the end of this section.

The positive direction of forces and angles is shown in figure 1.

A aspect ratio, b^2/S

b span, ft

c_f flap chord, ft

c_w wing chord, ft

C_D drag coefficient based on free-stream velocity, $\frac{\text{Drag}}{qS}$

C_L lift coefficient based on free-stream velocity, $\frac{L}{qS}$

$C_{L,s}$ lift coefficient based on slipstream velocity, $\frac{L}{q_s S}$; (designated C_L" in many of the references)

C_{L_α} lift-curve slope

C_T' propeller thrust coefficient based on free-stream velocity and wing area, $\frac{NT}{qS}$

$C_{T,s}$ propeller thrust coefficient based on slipstream velocity and propeller disk area, $\frac{T}{q_s S_p}$; (designated T_C" in many of the references)

C_X longitudinal-force coefficient based on free-stream velocity, $\frac{F_X}{qS}$

$C_{X,s}$ longitudinal-force coefficient based on slipstream velocity, $\frac{F_X}{q_s S}$; (designated C_X" in many of the references)

D propeller diameter, ft

D_O power-off wing drag, lb

d diameter of fully developed propeller slipstream, ft

e span efficiency factor

F resultant force, lb

F_X longitudinal force, lb

F/T thrust-recovery factor

i_w wing incidence, deg

k empirical constant for correcting lift-augmentation term

L	lift, lb
N	number of propellers
q	free-stream dynamic pressure, $\frac{\rho}{2}V^2$, lb/sq ft
q_s	slipstream dynamic pressure, used in this report as $q + \frac{T}{S_p}$, lb/sq ft
S	wing area, sq ft
S_p	propeller disk area, $\frac{\pi}{4}D^2$, sq ft
T	thrust per propeller or total thrust when used in thrust recovery factor F/T, lb
u	increment of velocity due to thrust in fully developed slipstream, ft/sec
V	free-stream velocity, ft/sec
ΔV	vector change in velocity, ft/sec
w	mass flow, slugs/sec
α	angle of attack measured between free-stream velocity and thrust axis; or, for hovering conditions, inclination of thrust axis above horizontal plane, deg
δ	flap deflection, deg
δ_e	equivalent flap deflection due to wing camber and incidence, deg
ϵ	downwash angle due to wing lift, deg
θ	slipstream turning angle, measured from thrust axis, deg
$\Delta\theta$	increment of turning angle due to wing camber and incidence, deg
ρ	air density, slugs/cu ft

Subscripts:

calc	calculated value
exp	experimental value
i	induced
max	maximum value
0	power-off conditions
s	slipstream

Conversion between systems:

$$C_D = \frac{-C_{X,s}}{1 - C_{T,s}}$$

$$C_L = \frac{C_{L,s}}{1 - C_{T,s}}$$

$$C_{L,s} = \frac{C_L}{1 + C_T' \frac{S}{NS_p}}$$

$$C_T' = \frac{C_{T,s}}{1 - C_{T,s}} \frac{NS_p}{S}$$

$$C_{T,s} = \frac{C_T'}{C_T' + \frac{NS_p}{S}}$$

$$C_{X,s} = \frac{-C_D}{1 + C_T' \frac{S}{NS_p}}$$

$$q = q_s(1 - C_{T,s})$$

DERIVATION OF EQUATIONS

Basis of Analysis

Heavier-than-air aircraft obtain lift by forcing air downward. A helicopter in hovering accelerates air downward by the action of its rotor. An airplane in cruising flight forces air downward with its wings. As assumed in the momentum theory, the mass flow of air deflected downward by a wing is that mass flow contained in the stream tube which has the wing span as its diameter.

Also, thrust is created by the action of the propellers in accelerating air rearward. If the slipstream, which is the stream tube accelerated by the propellers, is deflected downward (either by means of flaps or by tilting the thrust axis), a lift force is also obtained from this source - although at the expense of the loss of some of the force in the longitudinal direction. The flow system then for a wing-propeller combination can be thought of as consisting of two stream-tube systems as shown in the following diagram:

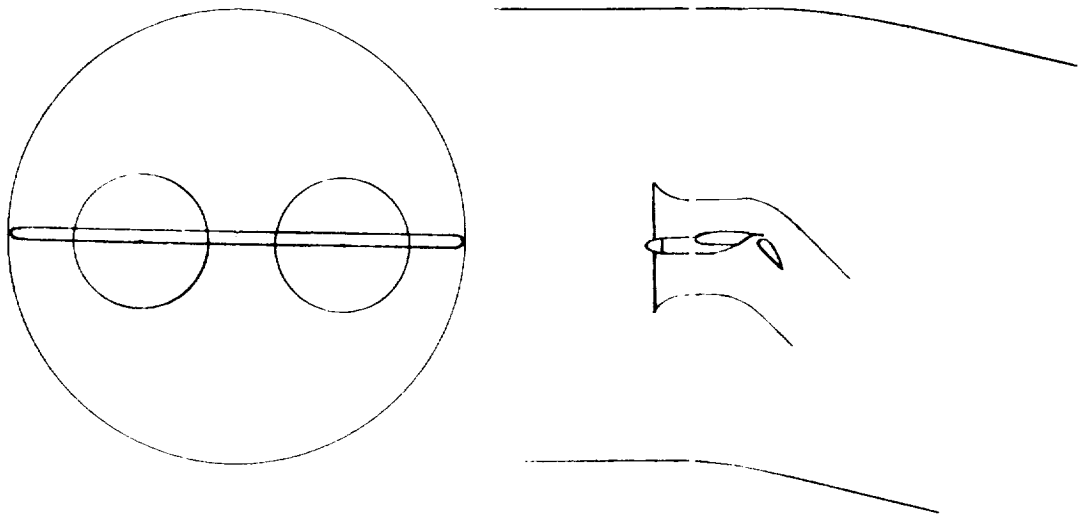

The larger stream tube is affected by the wing and is deflected through small to moderate angles for the most part. Contained within this larger stream tube are the smaller stream tubes which arise from the action of the propellers (referred to as the slipstream) and which can be deflected through large angles. Lift and drag (or thrust) forces arise from the acceleration and deflection of both of these systems of stream tubes. First, the forces arising from the deflection of each

stream-tube system are examined separately and then they are combined to arrive at a procedure for estimating the lift and drag characteristics of propeller-wing-flap configurations.

Power-Off Wing Characteristics

In the cruising and high-speed flight regime the contribution of the slipstreams to the lift can usually be considered negligible. In this case all the lift is obtained by the deflection of the larger stream tube and can be calculated conveniently with the simple momentum theory for wings. The momentum theory has been adequately treated in the literature. However, the fundamentals of the momentum theory as applied to wings are repeated herein for completeness and clarity in connection with the derivations for the power-off wing characteristics to follow.

The mass of air per unit time in the stream tube affected by the wing is given by

$$w = \frac{\pi}{4} b^2 \rho V$$

The stream tube with this mass flow is deflected through an angle ϵ and the change in velocity in the lift direction is

$$\Delta V = V \sin \epsilon$$

Thus the lift can be written as

$$L = \frac{\pi}{4} b^2 \rho V^2 \sin \epsilon \qquad (1)$$

At cruising speeds where the velocity V is large, the mass flow is very large and the lift necessary to support the airplane is produced with only a very small deflection of the stream tube. As the speed is reduced, however, the mass flow is reduced, and, in order to support the same weight, the air must be deflected through much larger angles. The problem of flying at very low speeds then involves turning the relatively low mass flow of air in the stream tube through large angles with a minimum of loss. The extrapolation of the momentum theory to large angles, as used herein, is simply an assumption, but

experience has indicated that the theory gives reasonably accurate results so long as stall can be avoided.

In the process of deflecting the stream tube downward, there is also a change in velocity in the drag direction. This change in velocity is given by

$$\Delta V = V - V \cos \epsilon$$

Thus the drag due to creating the lift is given by

$$\text{Drag} = \frac{\pi}{4} b^2 \rho V^2 (1 - \cos \epsilon) \tag{2}$$

Solving for V in equation (1), substituting the value into equation (2), using the small-angle assumption, and reducing to coefficient form leads to the following familiar induced-drag relation:

$$C_{D,i} = \frac{C_L^2}{\pi A}$$

The expressions for lift and drag presented herein (eqs. (1) and (2)) represent the high end of the speed range, and any procedure for calculating the lift and drag in the transition speed range should logically approach these expressions as the velocity is increased and the thrust reduced to zero.

Propeller-Slipstream Characteristics

At zero forward speed, only the slipstreams are available to produce lift. A considerable amount of experimental data on the effectiveness of wing-flap systems in deflecting propeller slipstreams is available. These data (which are summarized subsequently) are usually presented in terms of the turning angle θ and the thrust-recovery factor F/T. Thus, the total force is $\frac{F}{T}NT$ and the lift and longitudinal force are the components

$$L = \frac{F}{T} NT \sin(\theta + \alpha) \tag{3}$$

$$F_X = \frac{F_N}{T} T \cos(\theta + \alpha) \tag{4}$$

These expressions represent the conditions at the low end of the speed range. Any procedure for calculating the lift and drag in transition must approach these expressions as the speed is reduced to zero.

The propeller thrust and the characteristics of the slipstream at any speed can be calculated from the momentum theory for propellers, the details of which are also presented in this section for completeness and clarity.

The momentum theory as applied to propellers shows that one-half of the increment of velocity u attained in the fully developed slipstream is attained at the propeller disk. The mass flow through the propeller is then given by

$$w = \frac{\pi}{4} D^2 \rho \left(V + \frac{u}{2} \right)$$

and the thrust is given by

$$T = wu = \frac{\pi}{4} D^2 \rho \left(V + \frac{u}{2} \right) u \tag{5}$$

In order to simplify the analysis, the angle of attack α is assumed here to be small; therefore, there is no change in u with α. Solving for the velocity in the slipstream from equation (5) yields

$$u = -V \pm \sqrt{V^2 + \frac{T}{\frac{\rho}{2} \frac{\pi}{4} D^2}}$$

or

$$(V + u)^2 = V^2 + \frac{T}{\frac{\rho}{2} \frac{\pi}{4} D^2}$$

which may be expressed in terms of the dynamic pressure as

$$q_s = q + \frac{T}{S_p}$$

If thrust coefficient based on free-stream dynamic pressure and wing area is defined as

$$C_T' = \frac{NT}{qS}$$

then

$$q_s = q\left(1 + C_T'\frac{S}{NS_p}\right) \tag{6}$$

and

$$\frac{u}{V} = -1 + \sqrt{1 + C_T'\frac{S}{NS_p}} \tag{7}$$

The diameter d of the fully developed propeller slipstream can be determined from the equation for continuity as follows:

$$\frac{\pi}{4}D^2\rho\left(V + \frac{u}{2}\right) = \frac{\pi}{4}d^2\rho(V - u)$$

$$\frac{d^2}{D^2} = \frac{1 + \frac{u}{2V}}{1 + \frac{u}{V}} \tag{8}$$

Characteristics of Wing and Propeller in Combination

Lift in transition.- At intermediate speeds, both stream tubes must be considered in computing the lift and drag forces of the wing-propeller combination. The lift is given by the summation of the mass flows in the two stream-tube systems multiplied by their respective downward velocity components; that is, $L = \Sigma\rho\,\Delta V$. The mass flow in the total system is given by

$$w = N\frac{\pi}{4}D^2\rho\left(V + \frac{u}{2}\right) + \frac{\pi}{4}b^2\rho V - N\frac{\pi}{4}d^2\rho V \qquad (9)$$

where the first term represents the mass flow contained in N slipstreams and the second and third terms represent the mass flow in the main stream tube affected by the wing. The third term is necessary to correct for the fact that the slipstreams are occupying space within the larger wing stream tube. It is assumed here that the fully contracted slipstream diameter d is obtained at the wing. It is also assumed that the contraction of the propeller slipstreams did not alter the diameter of the stream tube affected by the wing.

The appropriate downward increment of velocity must now be applied to each term of equation (9) to calculate the lift. In order to make this calculation, the slipstreams are assumed to be deflected through the turning angle θ obtained at zero forward speed, and the larger stream tube affected by the wing is deflected through the downwash angle ϵ obtained under power-off conditions. Actually, the turning angle θ is probably decreased by the action of the main stream tube. Also the downwash angle ϵ may be increased somewhat by the action of the slipstreams, but recent unpublished data indicate that this effect may be small. Appropriate variations of θ and ϵ with speed and power are not available, however, and do not appear to be readily estimated. The assumption that θ and ϵ remain constant with changes in speed and power must therefore be made in order to arrive at a workable solution. The lift is then given by

$$L = \frac{F}{T}N\frac{\pi}{4}D^2\rho\left(V + \frac{u}{2}\right)(V + u)\sin(\theta + \alpha) + \frac{\pi}{4}b^2\rho V^2\sin\epsilon - \frac{F}{T}N\frac{\pi}{4}d^2\rho V^2\sin(\theta + \alpha) \qquad (10)$$

Note that the assumption that θ did not decrease with V has made necessary the arbitrary use of the factor $\sin(\theta + \alpha)$ in the last term of equation (10) instead of $\sin\epsilon$ which would appear logical. The use of the factor $\sin(\theta + \alpha)$ was necessary so that the equation would reduce to the expression for power-off lift under power-off conditions (eq. (1)).

Since in the first term of equation (10)

$$\frac{\pi}{4}D^2\rho\left(V + \frac{u}{2}\right)u = T$$

the expression for lift can be written as

$$L = L_O + \frac{F}{T}NT \sin(\theta + \alpha) + \frac{F}{T}N\frac{\pi}{4}D^2\rho V^2 \sin(\theta + \alpha)\left(1 + \frac{u}{2V} - \frac{d^2}{D^2}\right)$$

Reducing to coefficient form and substituting for $\frac{u}{V}$ and $\frac{d^2}{D^2}$ from equations (7) and (8) gives

$$C_L = C_{L,O} + \frac{F}{T}C_T' \sin(\theta + \alpha) + \frac{F}{T}C_T' \sin(\theta + \alpha)\frac{1}{\sqrt{1 + C_T'\frac{S}{NS_p}}} \qquad (11a)$$

where the first term represents the power-off lift contribution, the second term represents the direct thrust contribution, and the third term represents the lift augmentation on the wing due to the propeller slipstream. This augmentation arises from the increased mass flow in the system caused by the higher velocity in the propeller slipstream. The significance of these terms is illustrated in the following sketch:

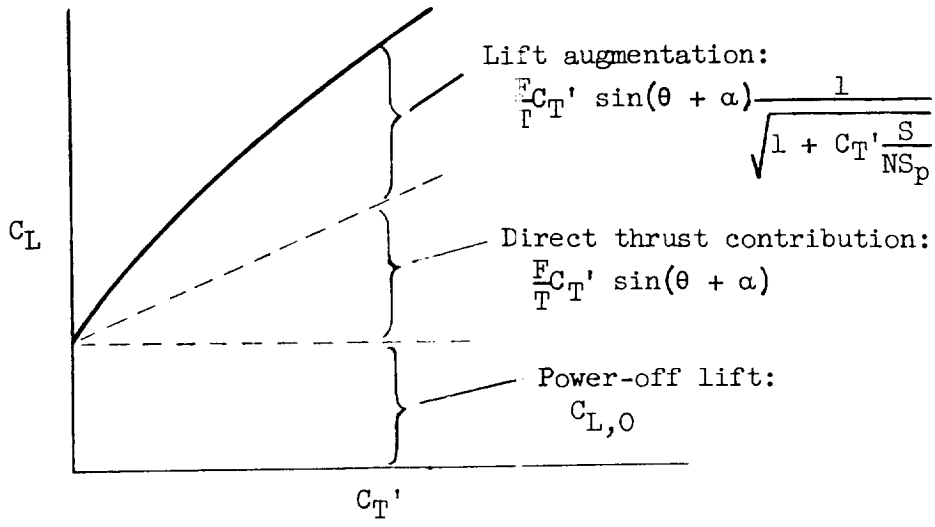

Equation (11a) can be presented in terms of the velocity in the slipstream as follows:

$$C_{L,s} = C_{L,0}(1 - C_{T,s}) + \frac{F}{T}C_{T,s} \sin(\theta + \alpha)\frac{NS_p}{S} + \frac{F}{T}C_{T,s} \sin(\theta + \alpha)\frac{NS_p}{S}\sqrt{1 - C_{T,s}} \qquad 11(b)$$

Again the significance of these terms is illustrated:

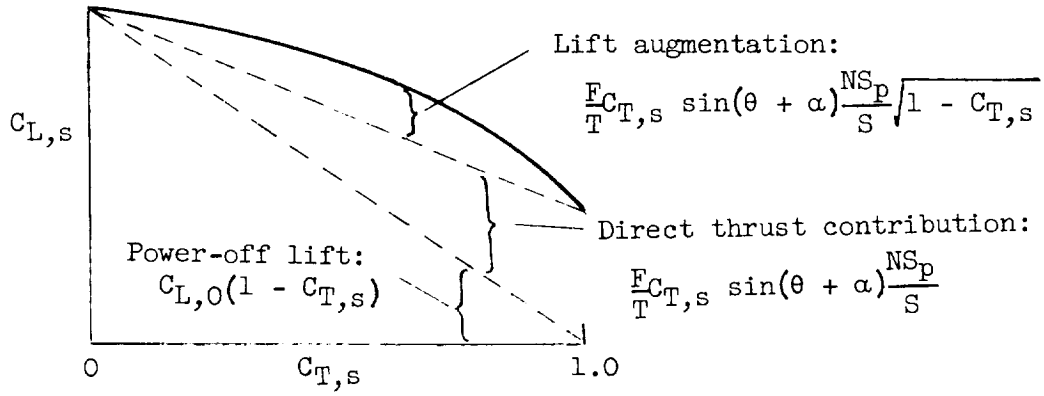

Lift-curve slope.- The lift-curve slope of the wing-propeller combination with flaps retracted ($\theta = 0$) can be obtained by dividing through by α, where α in this case is measured from the angle for zero lift. Thus, for small angles

$$C_{L_\alpha} = C_{L_\alpha,0} + \frac{F}{T}\frac{C_T'}{57.3} + \frac{F}{T}\frac{C_T'}{57.3}\frac{1}{\sqrt{1 + C_T'\frac{S}{NS_p}}} \qquad (12a)$$

or in terms of the velocity in the slipstream, rather than the free-stream velocity,

$$C_{L_{\alpha,s}} = C_{L_\alpha,0}(1 - C_{T,s}) + \frac{F}{T}\frac{C_{T,s}}{57.3}\frac{NS_p}{S} + \frac{F}{T}\frac{C_{T,s}}{57.3}\frac{NS_p}{S}\sqrt{1 - C_{T,s}} \qquad (12b)$$

where the first term again represents the power-off lift contribution, the second term represents the direct thrust contribution, and the third term represents the lift augmentation.

Drag or longitudinal force in transition.- The drag or longitudinal force can be estimated from the change in momentum in the longitudinal direction as follows:

$$F_X = \frac{F_N}{T}\frac{\pi}{4}D^2\rho\left(V + \frac{u}{2}\right)u - \frac{\pi}{4}b^2\rho V^2(1 - \cos\epsilon) -$$

$$\frac{F_N}{T}\frac{\pi}{4}D^2\rho\left(V + \frac{u}{2}\right)(V + u)\left[1 - \cos(\theta + \alpha)\right] + \frac{F_N}{T}\frac{\pi}{4}d^2\rho V^2\left[1 - \cos(\theta + \alpha)\right]$$

where the first term represents the thrust force arising from the action of the propeller in accelerating the air in the slipstream rearward, the second term represents the power-off wing drag D_0 (which should include the profile drag), the third term represents the drag component of the force required to deflect the mass flow of air in the propeller slipstreams, and the fourth term corrects for the fact that the slipstreams were developed from some of the mass flow contained in the larger stream tube and this increment of mass flow is included in both the second and third terms.

Again noting that

$$\frac{\pi}{4}D^2\rho\left(V + \frac{u}{2}\right)u = T$$

the longitudinal force can be written as

$$F_X = \frac{F_N}{T}T\cos(\theta + \alpha) - D_0 - \frac{F_N}{T}\frac{\pi}{4}D^2\rho V^2\left[1 - \cos(\theta + \alpha)\right]\left(1 + \frac{u}{2V} - \frac{d^2}{D^2}\right)$$

Reducing to coefficient form and substituting for $\frac{u}{V}$ and $\frac{d^2}{D^2}$ leads to the following equation:

$$C_X = \frac{F}{T}C_T'\cos(\theta + \alpha) - C_{D,0} - \frac{F}{T}C_T'\left[1 - \cos(\theta + \alpha)\right]\frac{1}{\sqrt{1 + C_T'\frac{S}{NS_p}}} \qquad (13a)$$

As was shown with the lift, the significance of these terms is illustrated in the following sketch:

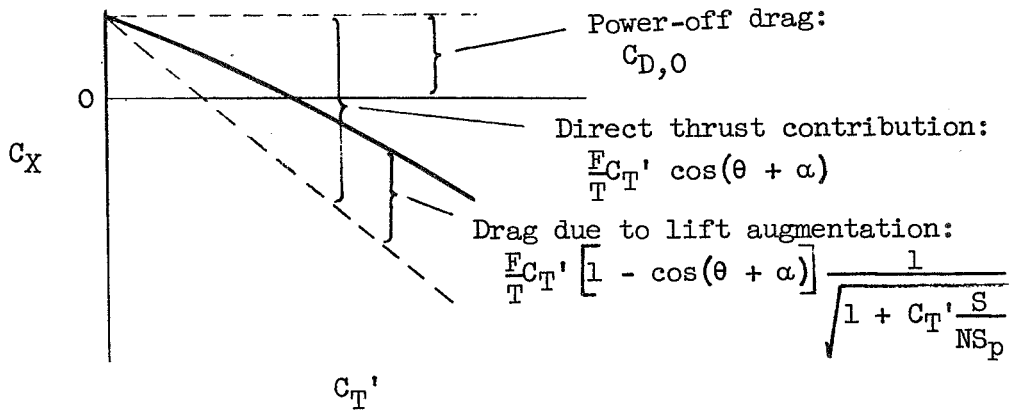

Equation (13a) in terms of the velocity in the slipstream becomes

$$C_{X,s} = \frac{F}{T}C_{T,s} \cos(\theta + \alpha)\frac{NS_p}{S} - C_{D,0}(1 - C_{T,s}) -$$

$$\frac{F}{T}C_{T,s} \left[1 - \cos(\theta + \alpha)\right] \frac{NS_p}{S}\sqrt{1 - C_{T,s}} \qquad (13b)$$

where the first term represents the component of thrust opposing the drag, the second represents the power-off drag contribution, and the third term represents the drag resulting from the lift augmentation due to slipstream. These terms can be illustrated as follows:

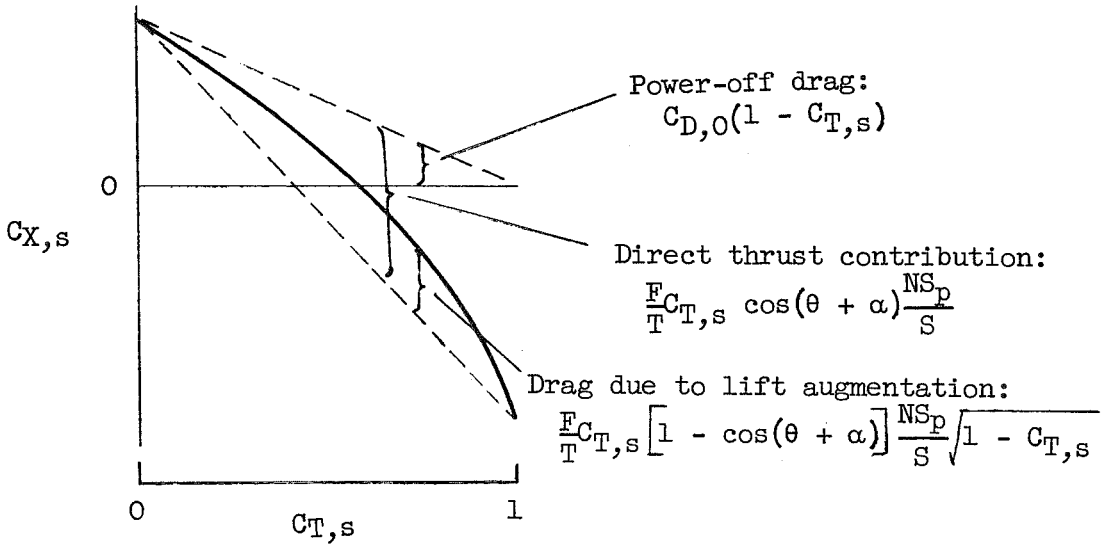

INFORMATION NECESSARY FOR APPLICATION OF EQUATIONS

In order to apply the equations developed in the previous sections, it is necessary to have or be able to estimate both the power-off lift and drag characteristics of the wing and the characteristics of the propeller wing-flap configuration at zero forward speed.

Estimation of Power-Off Data

Procedures for estimating the characteristics of wings in the absence of propeller slipstream (power off) have been extensively covered in the literature. However, special mention of some considerations with respect to these estimations must be made here.

The present analysis, of course, cannot predict the stall and only applies in the unstalled flight regime. The propeller slipstreams can reduce or eliminate stalling, particularly at high-power conditions. Therefore, a wing which is stalled in the power-off condition would frequently be unstalled at some moderate to high propeller thrust coefficient. In order to estimate properly the power-on data in this region, it is necessary to use the lift and drag values that would be reached if the wing were unstalled in the power-off condition. Where possible, the experimental power-off lift and drag data for the wing in question should be used and extrapolated for this purpose.

Configurations with large-chord flaps and large flap deflections frequently do not exhibit any region of unstalled flow in the power-off condition; that is, they are either stalled on the upper or on the lower surface throughout the angle-of-attack range. For such configurations, the lift must be estimated from the lift-curve slope and angle of attack for zero lift. The zero-lift angle of attack can be estimated from reference 22, for instance, and can reach high negative values for large flap deflections. Under these conditions the lift should be estimated as suggested in reference 22 by

$$C_L = C_{L_\alpha} 57.3 \sin(\alpha - \alpha_0)$$

The drag coefficient can be estimated from

$$C_{D,i} = \frac{C_L^2}{\pi A e}$$

where e is the span efficiency factor for the configuration.

Correlation of Slipstream Deflection Data

Turning angle.- The slipstream deflection characteristics at zero forward speed have been the subject of recent investigations as reported in references 2 to 10. When possible, the measured values of the turning angle θ and the thrust-recovery factor F/T for the flap configuration involved should be used. If appropriate data are not available for a particular configuration, the summary plots shown as figures 2 and 3 can be used to estimate θ and F/T or, preferably, they can be used to adjust the data from the closest available flap configuration for which data are available.

The turning angle θ has been found to be primarily a function of flap deflection, of the type of flap used, and of the ratio of the total extended flap chord to the propeller diameter. The turning angle per degree flap deflection θ/δ is shown in the left-hand plot of figure 2 and the maximum turning angle is shown in the right-hand plot. In using the slope θ/δ, it is necessary, of course, to be certain that one is working in the linear part of the curve of the variation of turning angle with flap deflection (sketch in upper right-hand corner). The slope is seen to be dependent only on the flap chord whereas the maximum turning angle is dependent both on flap chord and on the type of flap. In order to obtain high turning angles, it is necessary to use multiple flaps and either slots or large radii at the knee of the flap as illustrated by the sliding flaps (refs. 7 and 10). The effective aerodynamic chord of sliding flaps as used in figure 2 is measured to the knee of the sliding flaps.

The maximum turning angles shown have been adjusted to the condition of zero incidence and zero camber. Addition of incidence between the wing-chord plane and the thrust axis and the use of a cambered airfoil can increase the turning angle as indicated in references 4 and 7. This increment in turning angle can be estimated with reasonable accuracy for moderate cambers by first determining an equivalent flap deflection angle δ_e by measuring the angle between the thrust axis and the mean camber line at the wing trailing edge as indicated in the following sketch:

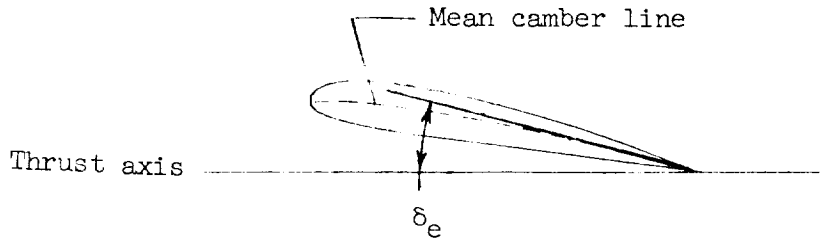

The increment of turning angle $\Delta\theta$ can be determined from figure 2 by assuming the wing to be a large-chord flap (that is, $c_w/D = c_f/D$) to determine θ/δ and by letting

$$\Delta\theta = \frac{\theta}{\delta}\delta_e$$

Thrust-recovery factor.- The thrust-recovery factor F/T (fig. 3) has been found to be a function of turning angle, flap configuration, and propeller arrangement. The best thrust recovery is obtained with the slotted flaps, probably because the slots provide for some boundary-layer cleanup. The sliding flaps give better thrust recovery than plain flaps because of the larger radii used at the knee of the flap and also because the turning process is started farther forward on the wing with the sliding flaps.

The single propeller per semispan provides the poorest recovery. The reasons for this are not fully known; however, flow studies have indicated that one contributing factor is the expansion of the slipstream in both directions under the wing. Overlapping two propellers so that their fully contracted slipstreams are tangent prevents this expansion between the slipstreams whereas using two propellers beside each other apparently allows some lateral loss between the slipstreams but not so much as a single slipstream. The use of strategically located fences on the wing lower surface can improve the thrust recovery somewhat by preventing some of this spanwise flow as indicated in references 7 and 11.

Overlapping the propellers also causes a reduction in the static-thrust efficiency of the propellers (ref. 10). The loss in thrust due to this reduced efficiency must be considered in evaluating the merits of propeller overlap.

Poor fairing between the nacelle and the wing (ref. 6) and large nacelles such as those that might be required for reciprocating engines can cause significant losses in thrust recovery and to a lesser extent in turning angle. The direction of propeller rotation also can have a significant effect on thrust recovery. References 3 and 7 indicate that for best recovery the outboard propellers should rotate so as to oppose the wing-tip vortex.

Large-chord leading-edge slats, such as those that might be used for pitching-moment and ground-effect relief (refs. 6, 7, and 10), can cause large losses in thrust recovery, particularly if positioned so as to produce large nose-up pitching moments.

COMPARISON OF ANALYSIS WITH EXPERIMENT

Comparison of experimental data with calculations made with the use of the analysis presented herein and in reference 23 are shown in figures 4 to 7. In making these calculations for the high-angle-of-attack cases, the power-off lift and drag data that would exist if the wing did not stall were used. Reference 23 adequately estimates the effects of slipstream on the lift of unflapped configurations (lift-curve slopes of fig. 6) at low thrust coefficients for which this reference was intended, but seriously underestimates the lift of flapped configurations (figs. 4 and 5). This result, which was anticipated by reference 23, arises primarily because the direct thrust contribution to lift is taken as the thrust multiplied by the sine of the angle of attack ($T \sin \alpha$); whereas, the present analysis indicates that the slipstream deflection angle should be included and the direct thrust contribution given by $L = T \sin(\theta + \alpha)$.

In general, the data calculated by the present method (eqs. (11)) also underestimate the lift somewhat. The simplifying assumption that θ and ϵ are constant is probably responsible for part of this disagreement. In order to obtain better agreement with the experimental data, an experimentally derived constant (designated k) can be introduced into the lift-augmentation term. The experimentally determined increments of lift due to slipstream have been plotted against their corresponding calculated values to determine this constant. The value of k is shown to be about 1.6 in figure 7. Considerable scatter occurs in the data in this plot, which may indicate the effect of the assumptions made in the analysis. Some of this scatter may also be due to experimental inaccuracy in the forward-speed data. It should be noted that reference 24 indicated that the proximity of the tunnel walls could affect the data obtained on configurations which deflect the slipstream through large angles unless the model is very small with respect to the tunnel. Although the experimental data used here are from configurations that did not involve very large turning angles, the models could not be considered to be very small with respect to tunnel size and therefore it cannot be stated with certainty that the experimental data are completely free of tunnel-wall effects. For this reason, attempting to find a more refined explanation of the scatter shown appears to have little justification at this time and it is suggested that the value of $k = 1.6$ be used until better and more comprehensive experimental evidence is available.

The constant k must, of course, also be applied to the increment of drag due to lift augmentation. The resulting equations then appear in terms of coefficients based on the free-stream dynamic pressure or based on the slipstream dynamic pressure as follows:

For lift coefficient,

$$C_L = C_{L,0} + \frac{F}{T}C_T' \sin(\theta + \alpha) + k\frac{F}{T}C_T' \sin(\theta + \alpha)\frac{1}{\sqrt{1 + C_T'\frac{S}{NS_p}}} \quad (14a)$$

or

$$C_{L,s} = C_{L,0}(1 - C_{T,s}) + \frac{F}{T}C_{T,s} \sin(\theta + \alpha)\frac{NS_p}{S} +$$

$$k\frac{F}{T}C_{T,s} \sin(\theta + \alpha)\frac{NS_p}{S}\sqrt{1 - C_{T,s}} \quad (14b)$$

for lift-curve slope,

$$C_{L_\alpha} = C_{L_\alpha,0} + \frac{F}{T}\frac{C_T'}{57.3} + k\frac{F}{T}\frac{C_T'}{57.3}\frac{1}{\sqrt{1 + C_T'\frac{S}{NS_p}}} \quad (15a)$$

or

$$C_{L_{\alpha,s}} = C_{L_\alpha,0}(1 - C_{T,s}) + \frac{F}{T}\frac{C_{T,s}}{57.3}\frac{NS_p}{S} + k\frac{F}{T}\frac{C_{T,s}}{57.3}\sqrt{1 - C_{T,s}}\frac{NS_p}{S} \quad (15b)$$

and, for longitudinal-force coefficient,

$$C_X = \frac{F}{T}C_T' \cos(\theta + \alpha) - C_{D,0} - k\frac{F}{T}C_T'\left[1 - \cos(\theta + \alpha)\right]\frac{1}{\sqrt{1 + C_T'\frac{S}{NS_p}}} \quad (16a)$$

or

$$C_{X,s} = \frac{F}{T}C_{T,s} \cos(\theta + \alpha)\frac{NS_p}{S} - C_{D,0}(1 - C_{T,s}) -$$

$$k\frac{F}{T}C_{T,s}\left[1 - \cos(\theta + \alpha)\right]\frac{NS_p}{S}\sqrt{1 - C_{T,s}} \quad (16b)$$

An additional comparison of the calculated values of lift coefficient and longitudinal-force coefficient (eqs. (14) and (16), $k = 1.6$) with

experimental data on a model that may be considered more representative of a VTOL configuration is presented in figure 8. These data were not used in the determination of the factor k and are recently obtained unpublished results from tests of the model of reference 10 in the 17-foot test section of the Langley 300-MPH 7- by 10-foot tunnel. Because of the large ratio of tunnel size to model size, these data are believed to be relatively free of tunnel-wall effects. The data are presented here as lift coefficient plotted against angle of attack and longitudinal-force coefficient in order to give an idea of the applicability of the estimating procedure at flight conditions of interest to VTOL and STOL airplanes. The thrust coefficients chosen represent high-power low-speed conditions well within the transition speed range. In these plots, the zero value of C_X indicates steady level flight, positive values indicate accelerating or climbing flight, and negative values indicate decelerating or landing approach conditions. Thus, the range of interest is in the region of zero longitudinal-force coefficient, and it is seen that, in general, for steady level flight and for climbing flight the estimating procedure gives reasonably good results. In the approach range (negative values of C_X), however, this particular wing stalls and poor agreement is shown. Also, at the extreme negative angles of attack, poor agreement results from stalling on the wing lower surface.

The fact that the lift—longitudinal-force polar for the largest flap deflection (fig. 8(c)) shows lower values of lift and longitudinal force than the similar configuration with a smaller flap deflection (fig. 8(b)) indicates that the wing with this large flap deflection (fig. 8(c)) was probably partly stalled throughout the angle-of-attack range. The disagreement shown here may also be an indication of the limits of application of the calculating procedure as presented here. Additional comparisons with data for other configurations will have to be made as the data become available before the full limits of application of the present method can be established.

Reference 25 on the lift and induced drag associated with large downwash angles is a related theoretical paper which became available after the completion of the present study.

CONCLUDING REMARKS

The semiempirical procedure for calculating the lift and drag of propeller-wing-flap configurations that would be suitable for VTOL and STOL airplanes is shown to give reasonably good agreement with experimental data. The procedure is applicable, however, only in the

unstalled flight regime; nevertheless, it should be useful in preliminary design estimates of the performance that may be expected of VTOL or STOL airplanes.

Langley Research Center,
National Aeronautics and Space Administration,
Langley Field, Va., October 7, 1958.

REFERENCES

1. Kuhn, Richard E., and Draper, John W.: Investigation of the Aerodynamic Characteristics of a Model Wing-Propeller Combination and of the Wing and Propeller Separately at Angles of Attack up to 90°. NACA Rep. 1263, 1956. (Supersedes NACA TN 3304 by Draper and Kuhn.)

2. Kuhn, Richard E., and Draper, John W.: An Investigation of a Wing-Propeller Configuration Employing Large-Chord Plain Flaps and Large-Diameter Propellers for Low-Speed Flight and Vertical Take-Off. NACA TN 3307, 1954.

3. Draper, John W., and Kuhn, Richard E.: Some Effects of Propeller Operation and Location on Ability of a Wing With Plain Flaps to Deflect Propeller Slipstreams Downward for Vertical Take-Off. NACA TN 3360, 1955.

4. Kuhn, Richard E., and Draper, John W.: Investigation of Effectiveness of Large-Chord Slotted Flaps in Deflecting Propeller Slipstreams Downward for Vertical Take-Off and Low-Speed Flight. NACA TN 3364, 1955.

5. Kuhn, Richard E.: Investigation of the Effects of Ground Proximity and Propeller Position on the Effectiveness of a Wing with Large-Chord Slotted Flaps in Redirecting Propeller Slipstreams Downward for Vertical Take-Off. NACA TN 3629, 1956.

6. Kuhn, Richard E.: Investigation at Zero Forward Speed of a Leading-Edge Slat as a Longitudinal Control Device for Vertically Rising Airplanes That Utilize the Redirected-Slipstream Principle. NACA TN 3692, 1956.

7. Kuhn, Richard E.: Investigation of Effectiveness of a Wing Equipped With a 30-Percent-Chord Sliding Flap, a 30-Percent-Chord Slotted Flap, and a 30-Percent-Chord Slat in Deflecting Propeller Slipstreams Downward for Vertical Take-Off. NACA TN 3919, 1957.

8. Spreemann, Kenneth P.: Investigation of the Effects of Propeller Diameter on the Ability of a Flapped Wing, With and Without Boundary-Layer Control, to Deflect a Propeller Slipstream Downward for Vertical Take-Off. NACA TN 4181, 1957.

9. Spreemann, Kenneth P.: Effectiveness of Boundary-Layer Control, Obtained by Blowing Over a Plain Rear Flap in Combination With a Forward Slotted Flap, in Deflecting a Slipstream Downward for Vertical Take-Off. NACA TN 4200, 1958.

10. Hayes, William C., Jr., Kuhn, Richard E., and Sherman, Irving R.: Effects of Propeller Position and Overlap on the Slipstream Deflection Characteristics of a Wing-Propeller Configuration Equipped With a Sliding and Fowler Flap. NACA TN 4404, 1958.

11. Kirby, Robert H.: Exploratory Investigation of the Effectiveness of Biplane Wings With Large-Chord Double Slotted Flaps in Redirecting a Propeller Slipstream Downward for Vertical Take-Off. NACA TN 3800, 1956.

12. Newsom, William A., Jr.: Effect of Propeller Location and Flap Deflection on the Aerodynamic Characteristics of a Wing-Propeller Combination for Angles of Attack From 0° to 80°. NACA TN 3917, 1957.

13. Tosti, Louis P., and Davenport, Edwin E.: Hovering Flight Tests of a Four-Engine-Transport Vertical Take-Off Airplane Model Utilizing a Large Flap and Extensible Vanes for Redirecting the Propeller Slipstream. NACA TN 3440, 1955.

14. Lovell, Powell M., Jr., and Parlett, Lysle P.: Hovering-Flight Tests of a Model of a Transport Vertical-Take-Off Airplane With Tilting Wing and Propellers. NACA TN 3630, 1956.

15. Lovell, Powell M., Jr., and Parlett, Lysle P.: Flight Tests of a Model of a High-Wing Transport Vertical-Take-Off Airplane With Tilting Wing and Propellers and With Jet Controls at the Rear of the Fuselage for Pitch and Yaw Control. NACA TN 3912, 1957.

16. Lovell, Powell M., Jr., and Parlett, Lysle P.: Transition-Flight Tests of a Model of a Low-Wing Transport Vertical-Take-Off Airplane With Tilting Wing and Propellers. NACA TN 3745, 1956.

17. Newsom, William A., Jr.: Effect of Ground Proximity on the Aerodynamic Characteristics of a Four-Engine Vertical-Take-Off-and-Landing Transport-Airplane Model With Tilting Wing and Propellers. NACA TN 4124, 1957.

18. Newsom, William A., Jr.: Experimental Investigation of the Lateral Trim of a Wing-Propeller Combination at Angles of Attack up to 90° With All Propellers Turning in the Same Direction. NACA TN 4190, 1958.

19. Tosti, Louis P.: Transition-Flight Investigation of a Four-Engine-Transport Vertical-Take-Off Airplane Model Utilizing a Large Flap and Extensible Vanes for Redirecting the Propeller Slipstream. NACA TN 4131, 1957.

20. Brenckmann, Marc E.: Experimental Investigation of the Aerodynamics of a Wing in a Slipstream. Jour. Aero. Sci., vol. 25, no. 5, May 1958, pp. 324-328.

21. Kuhn, Richard E.: Take-Off and Landing Distance and Power Requirements of Propeller-Driven STOL Airplanes. Aero. Eng. Rev., vol. 16, no. 11, Nov. 1957, pp. 38-42.

22. Keune, F.: Lift on a Bent, Flat Plate. NACA TM 1340, 1955.

23. Smelt, R., and Davies, H.: Estimation of Increase in Lift Due to Slipstream. R. & M. No. 1788, British A.R.C., 1937.

24. Kuhn, Richard E., and Hayes, William C., Jr.: Wind-Tunnel Investigation of Effect of Propeller Slipstreams on Aerodynamic Characteristics of a Wing Equipped With a 50-Percent-Chord Sliding Flap and a 30-Percent-Chord Slotted Flap. NACA TN 3918, 1957.

25. Ribner, H. S.: On the Lift and Induced Drag Associated With Large Downwash Angles. UTIA Tech. Note No. 19, Univ. of Toronto, Inst. Aerophysics, Jan. 1958.

26. Sleeman, William C., Jr., and Linsley, Edward L.: Low-Speed Wind-Tunnel Investigation of the Effects of Propeller Operation at High Thrust on the Longitudinal Stability and Trim of a Twin-Engine Airplane Configuration. NACA RM L52D04, 1952.

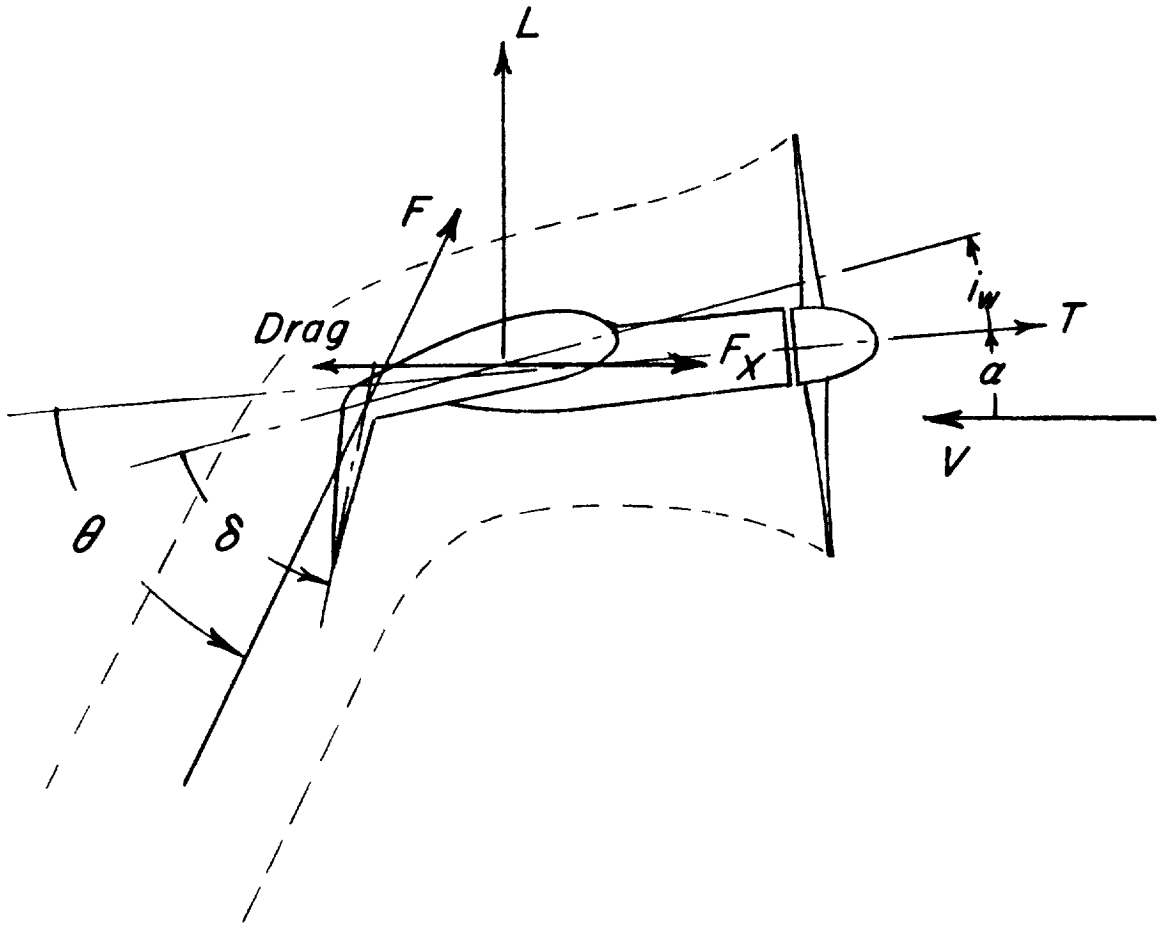

Figure 1.- Conventions used to define positive sense of forces and angles.

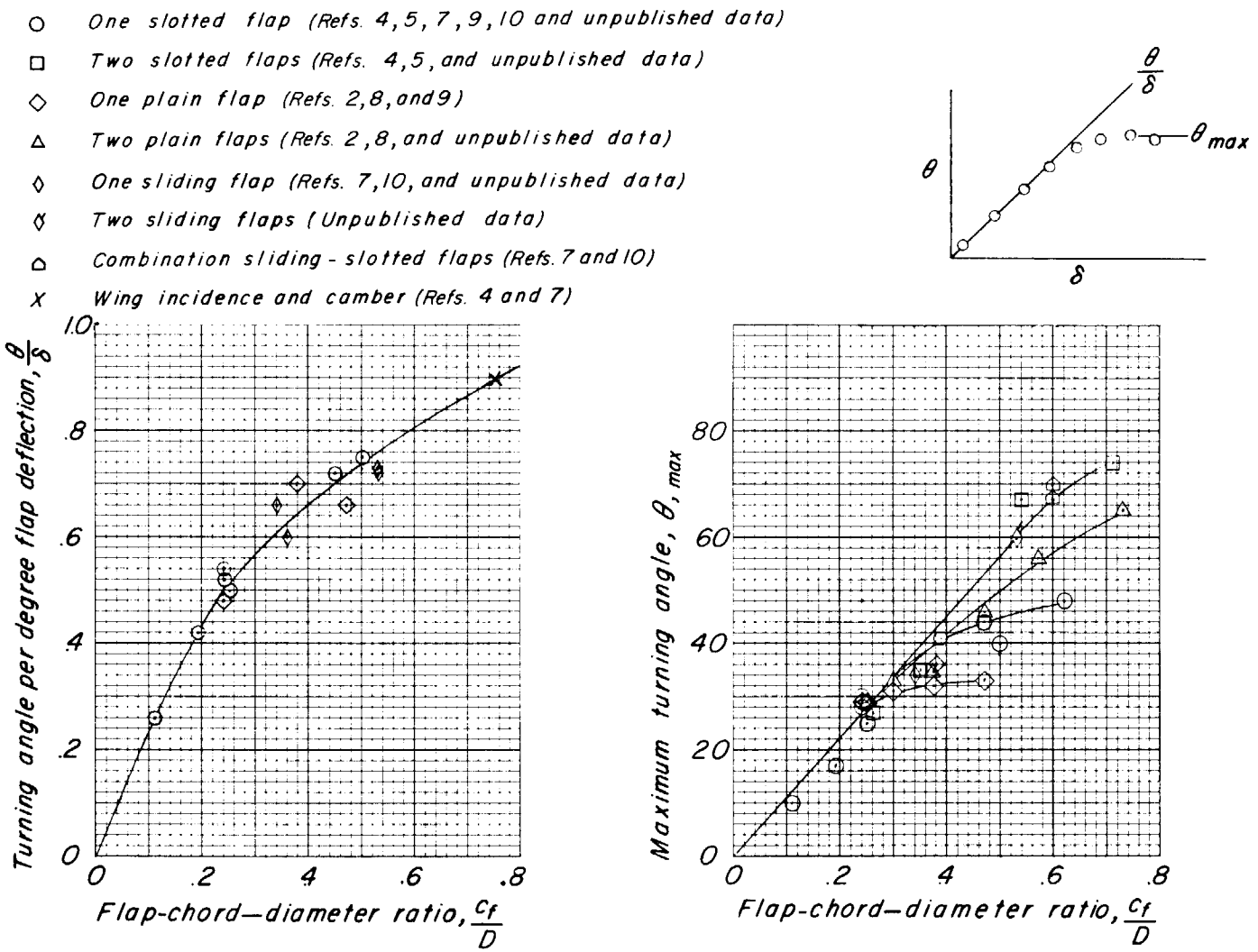

Figure 2.- Variation of turning angle with the ratio of total flap chord to propeller diameter for various flap configurations in hovering out of ground-effect region.

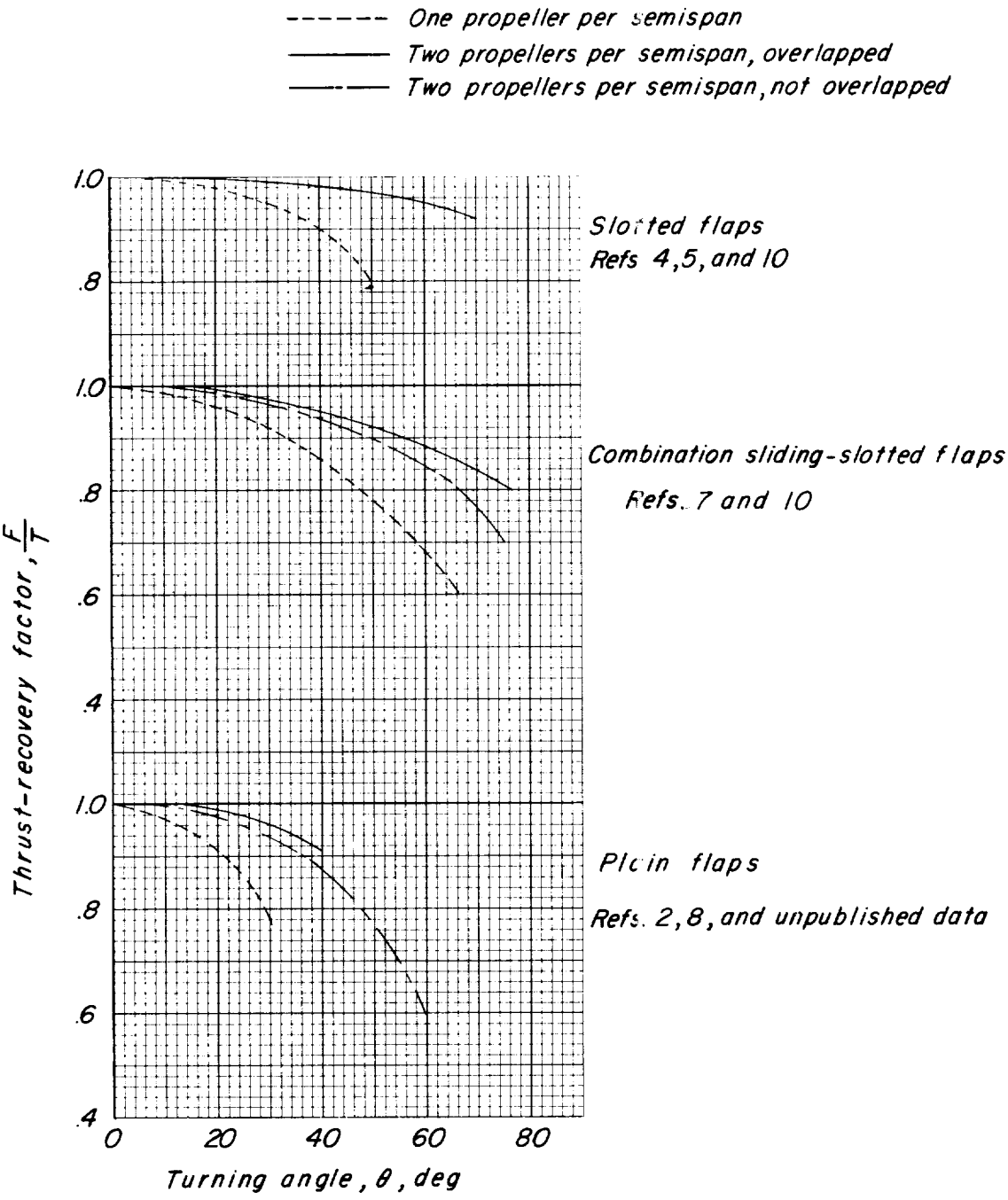

Figure 3.- Variation of the average thrust-recovery factor F/T for various flap and propeller configurations in hovering out of ground-effect region.

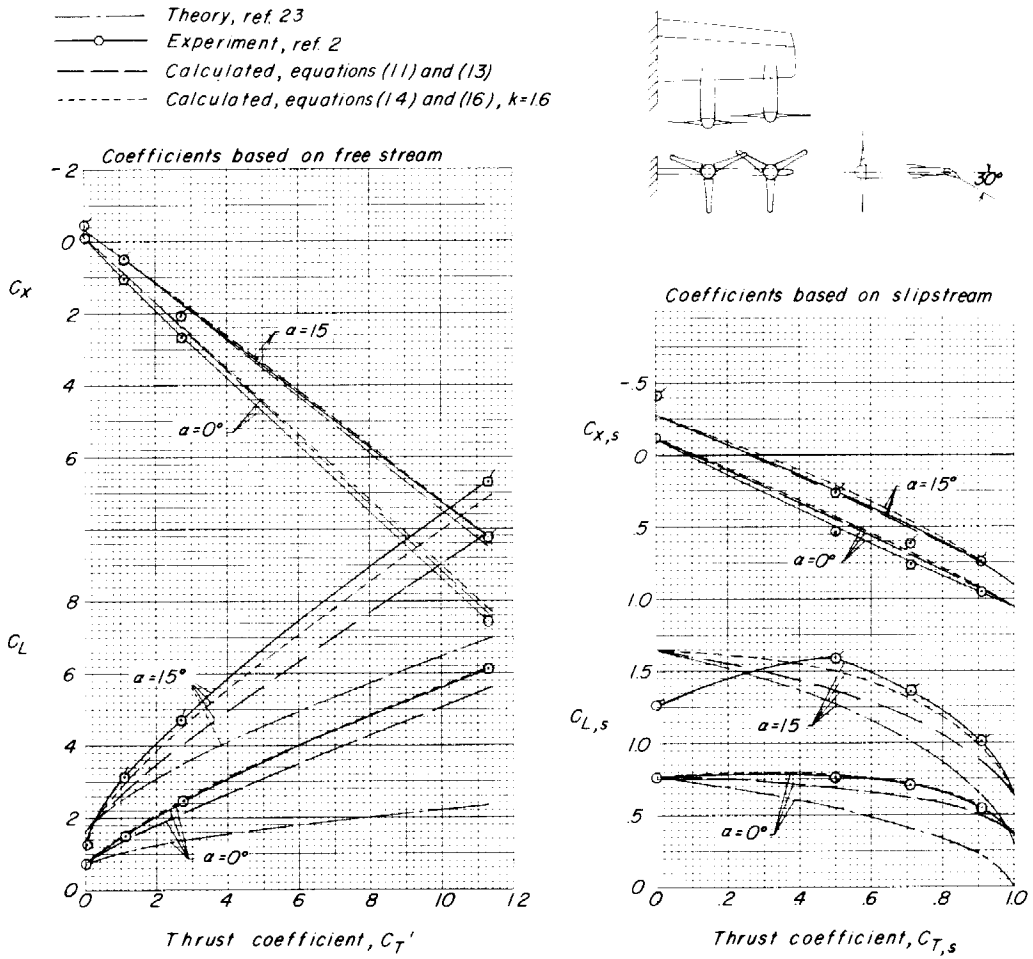

(a) Two propellers; $\delta = 30^\circ$.

Figure 4.- Comparison of calculated and experimental longitudinal-force and lift coefficients for a wing with a plain flap.

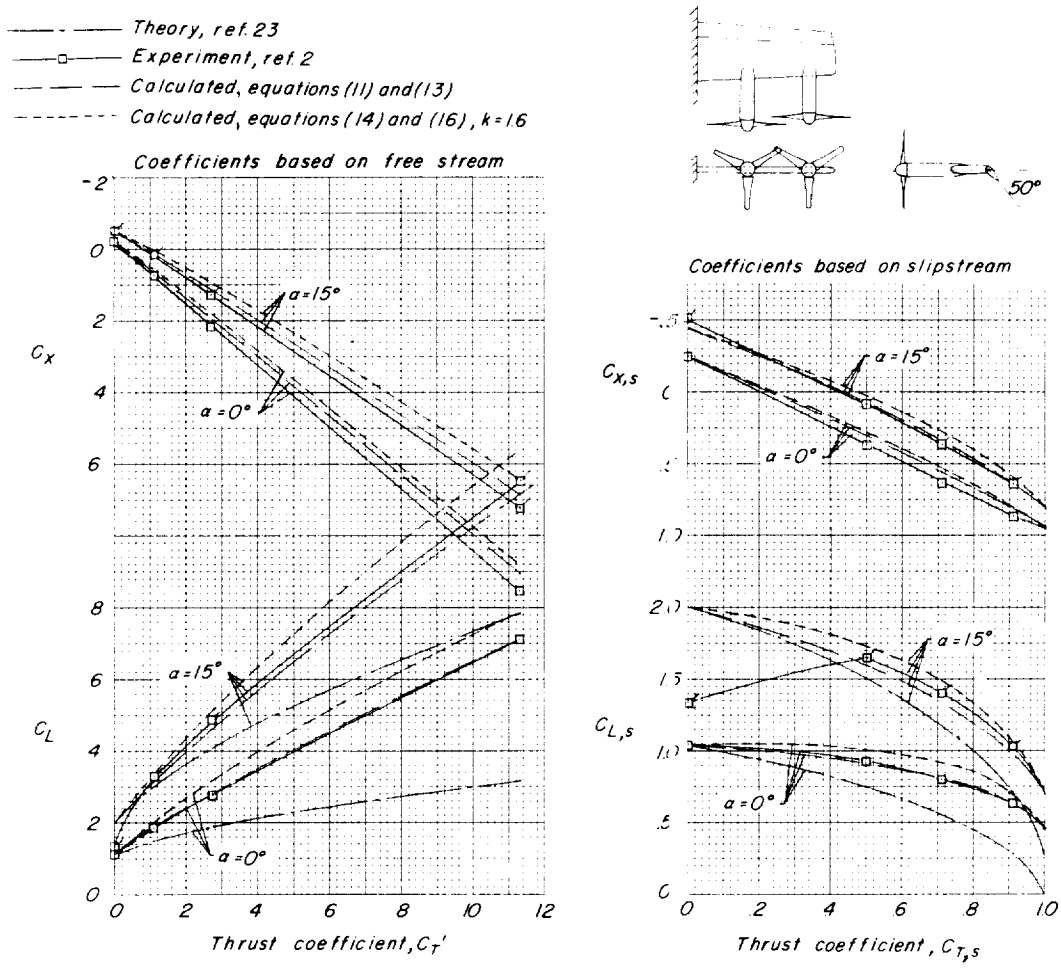

(b) Two propellers; δ = 50°.

Figure 4.- Continued.

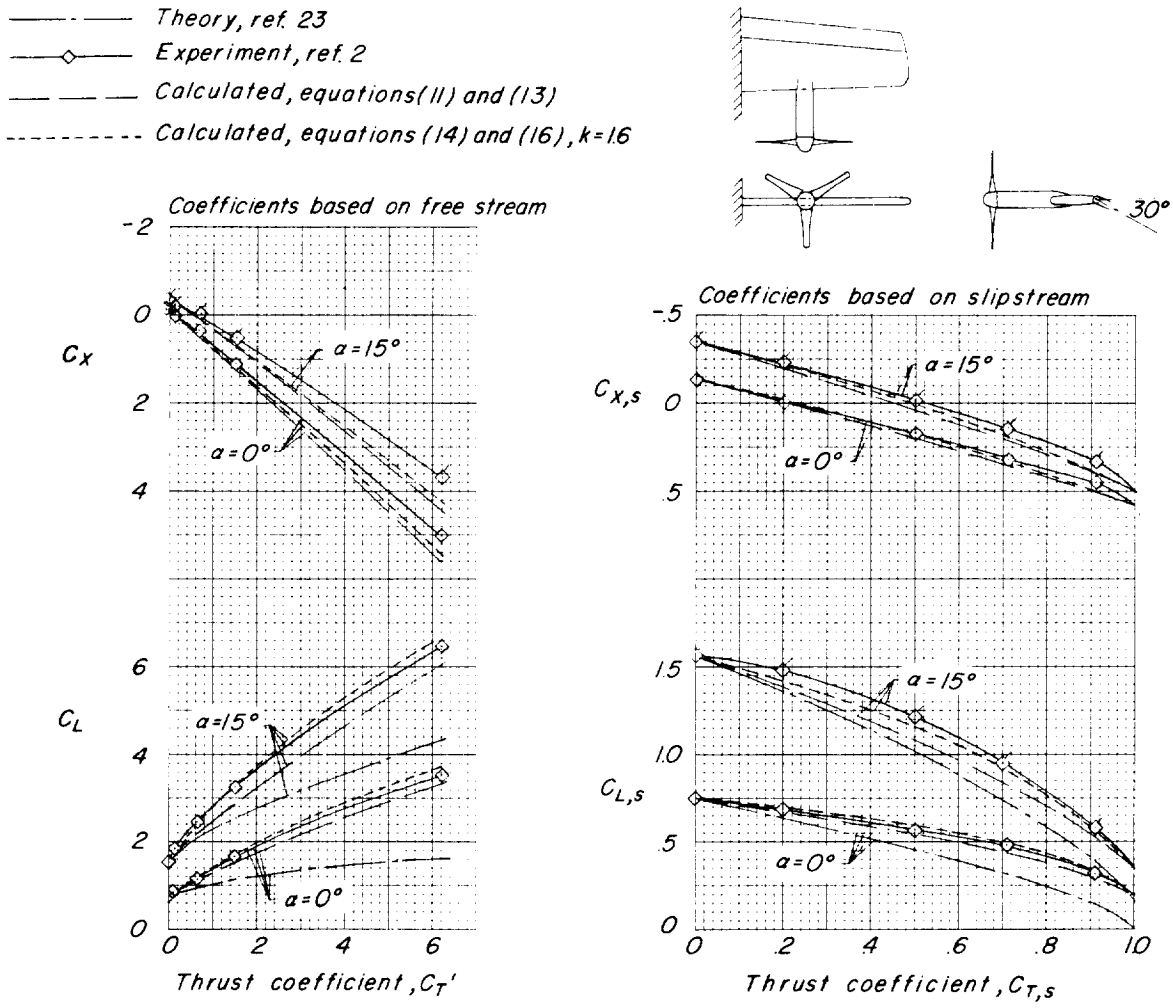

(c) One propeller; $\delta = 30^\circ$.

Figure 4.- Concluded.

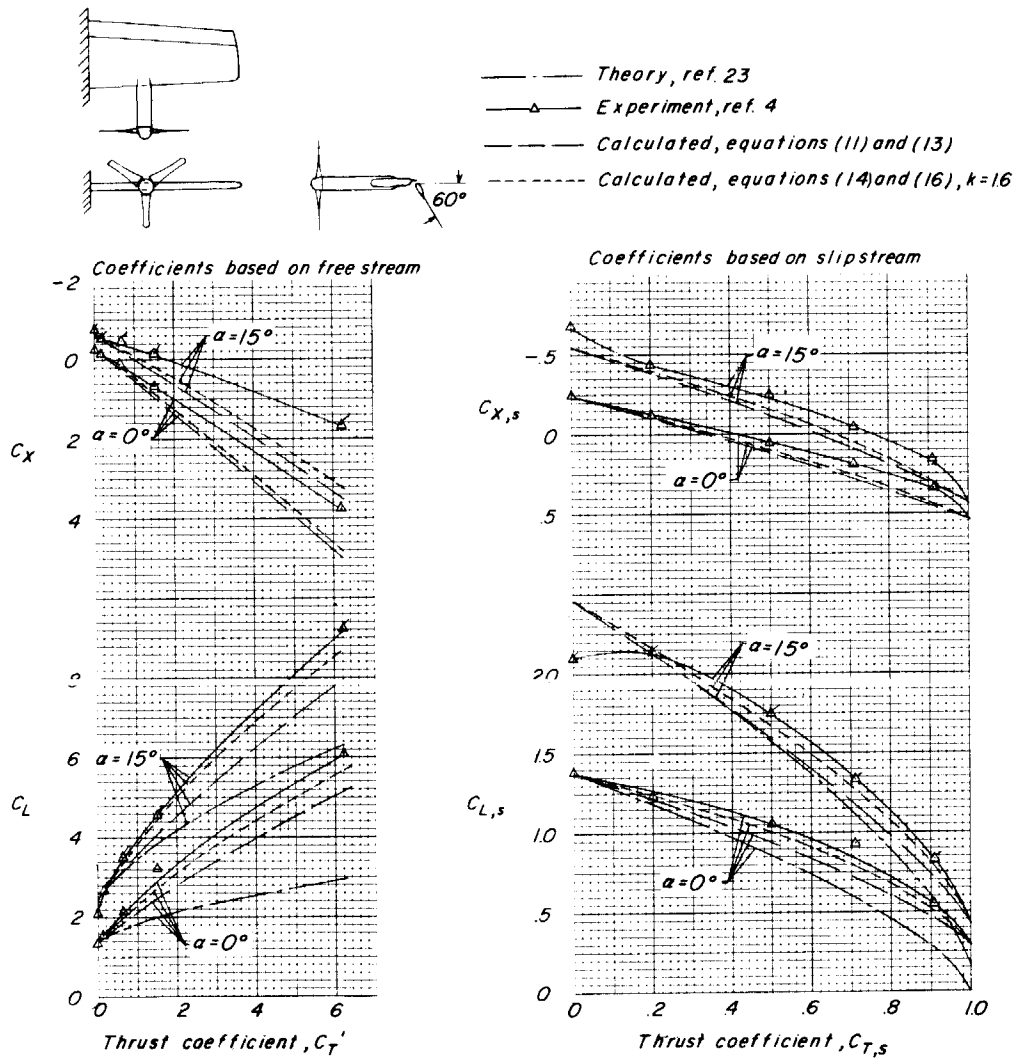

Figure 5.- Comparison of calculated and experimental longitudinal-force and lift coefficients for a wing with a slotted flap. One propeller; $\delta = 60^\circ$.

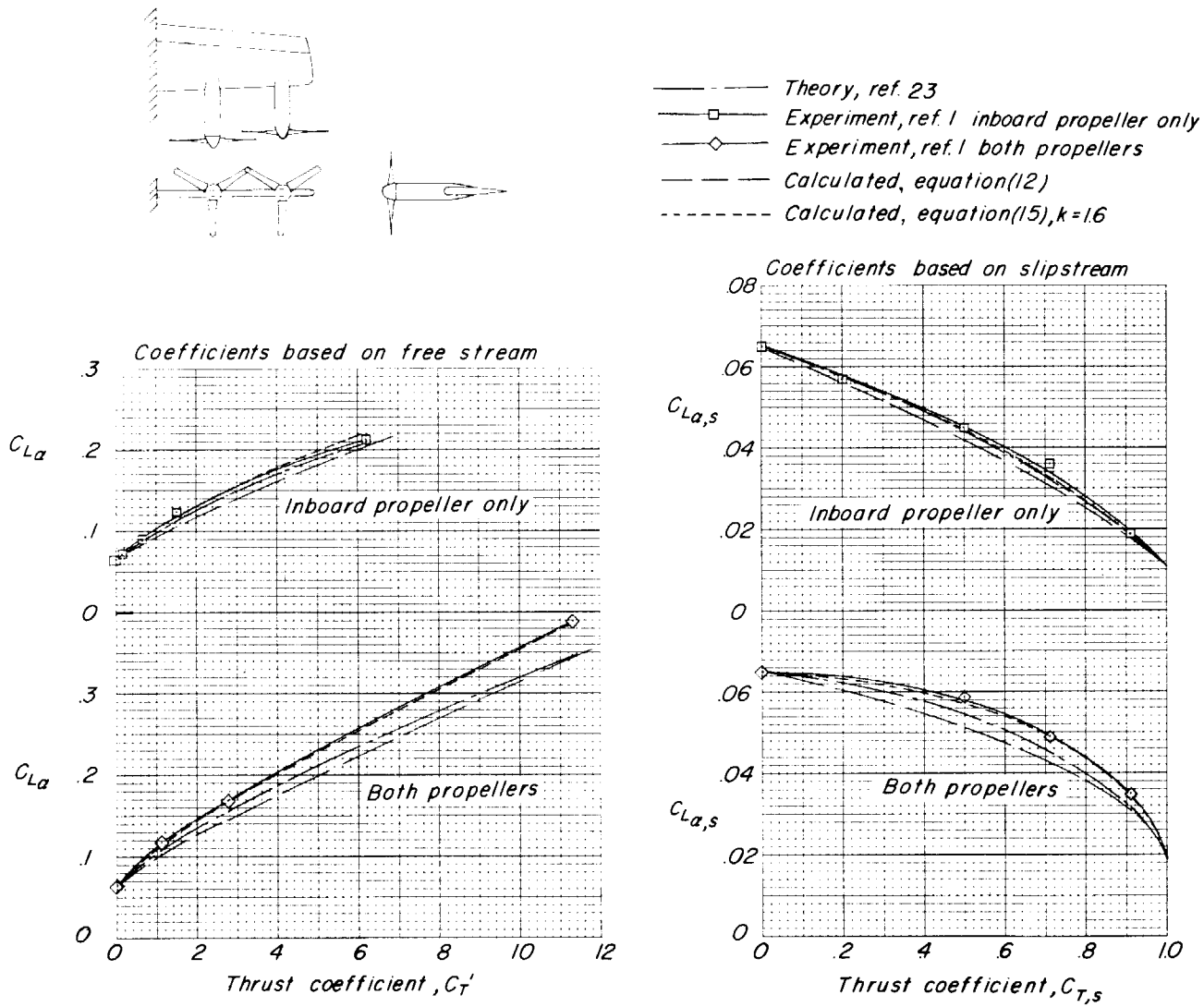

Figure 6.- Comparison of calculated and experimental lift-curve slopes.

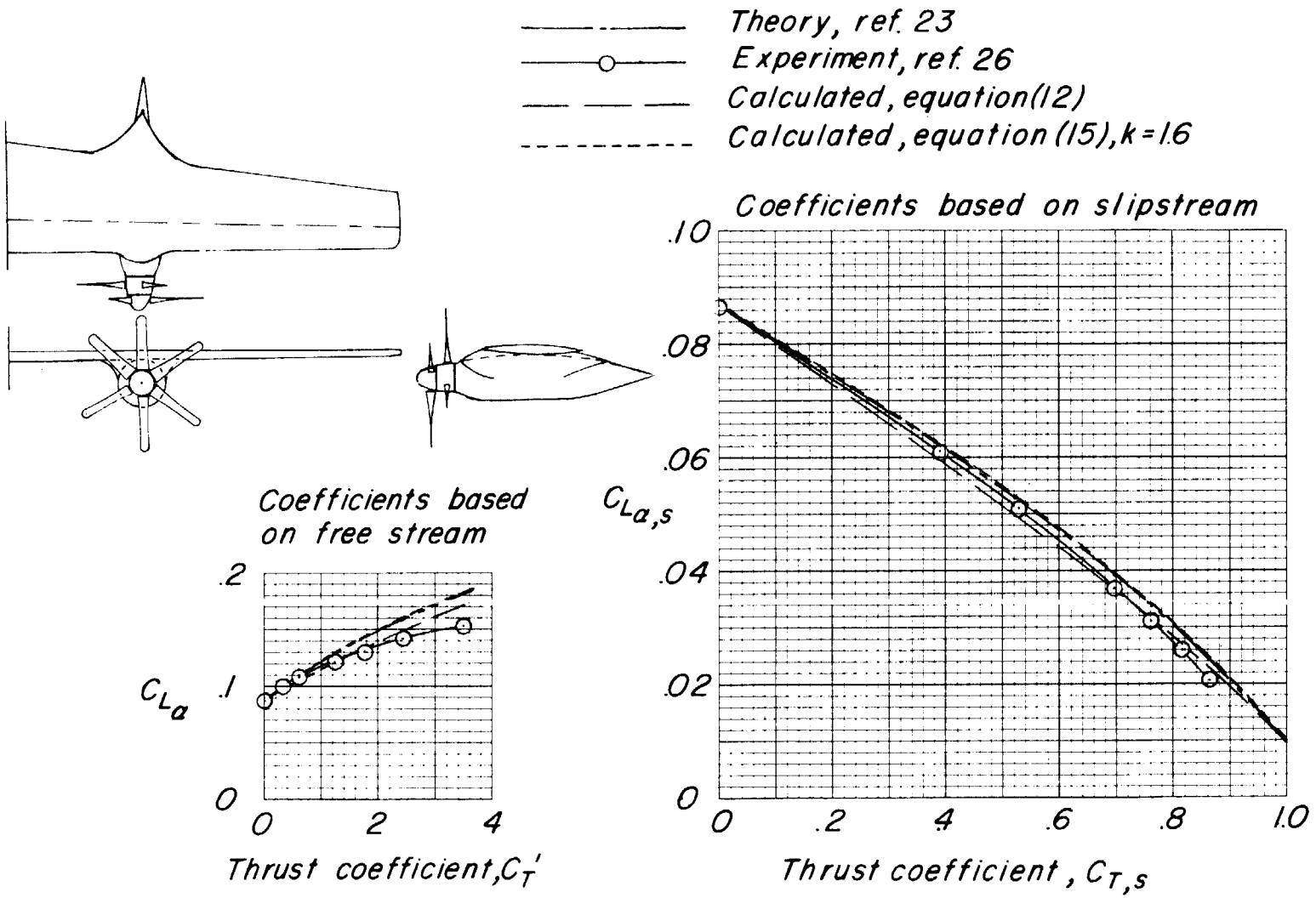

Figure 6.- Concluded.

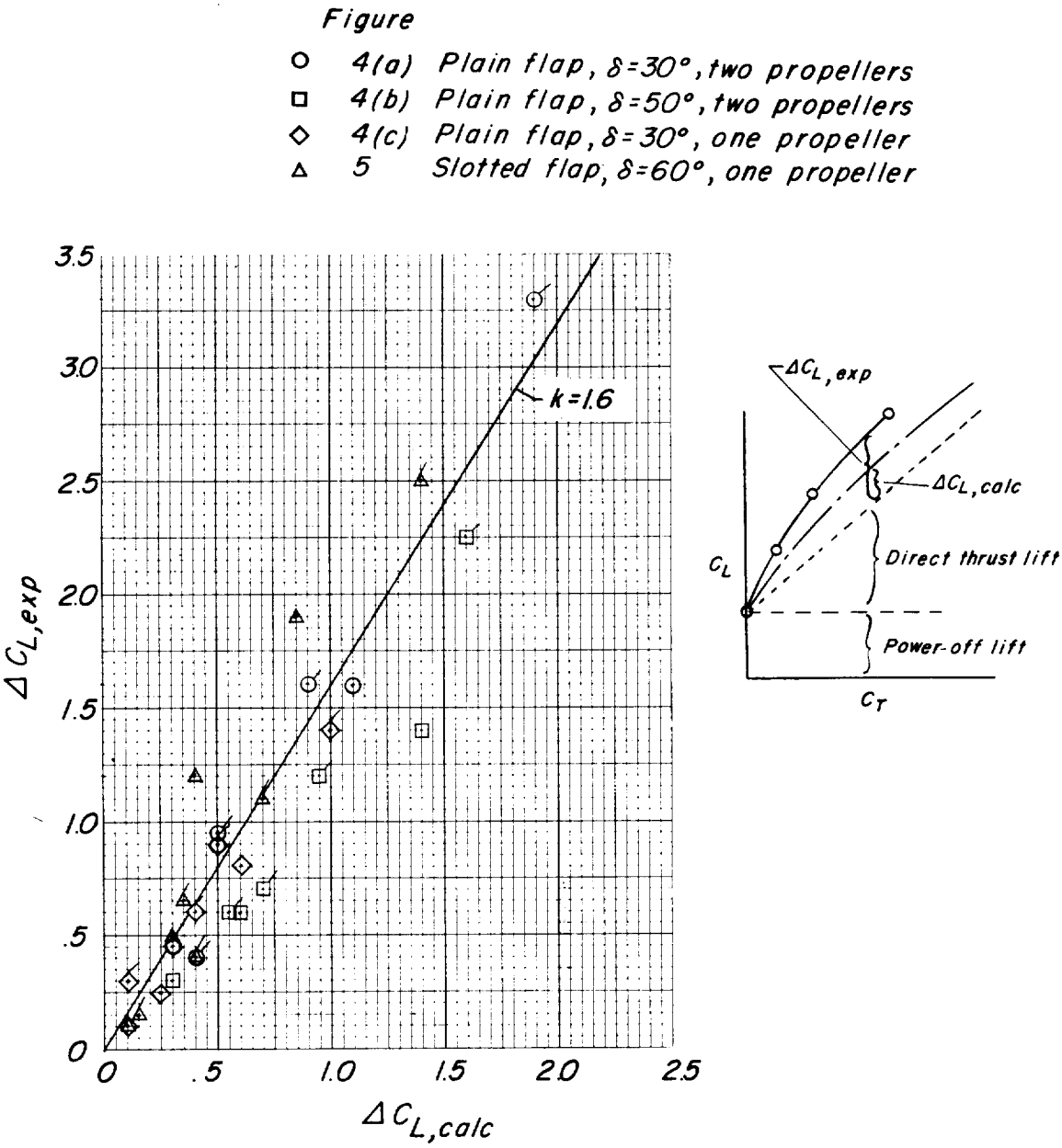

Figure 7.- Correlation of calculated and experimental increments of lift augmentation due to propeller slipstream. (Flagged symbols indicate $\alpha = 15^{\circ}$; unflagged symbols indicate $\alpha = 0^{\circ}$.)

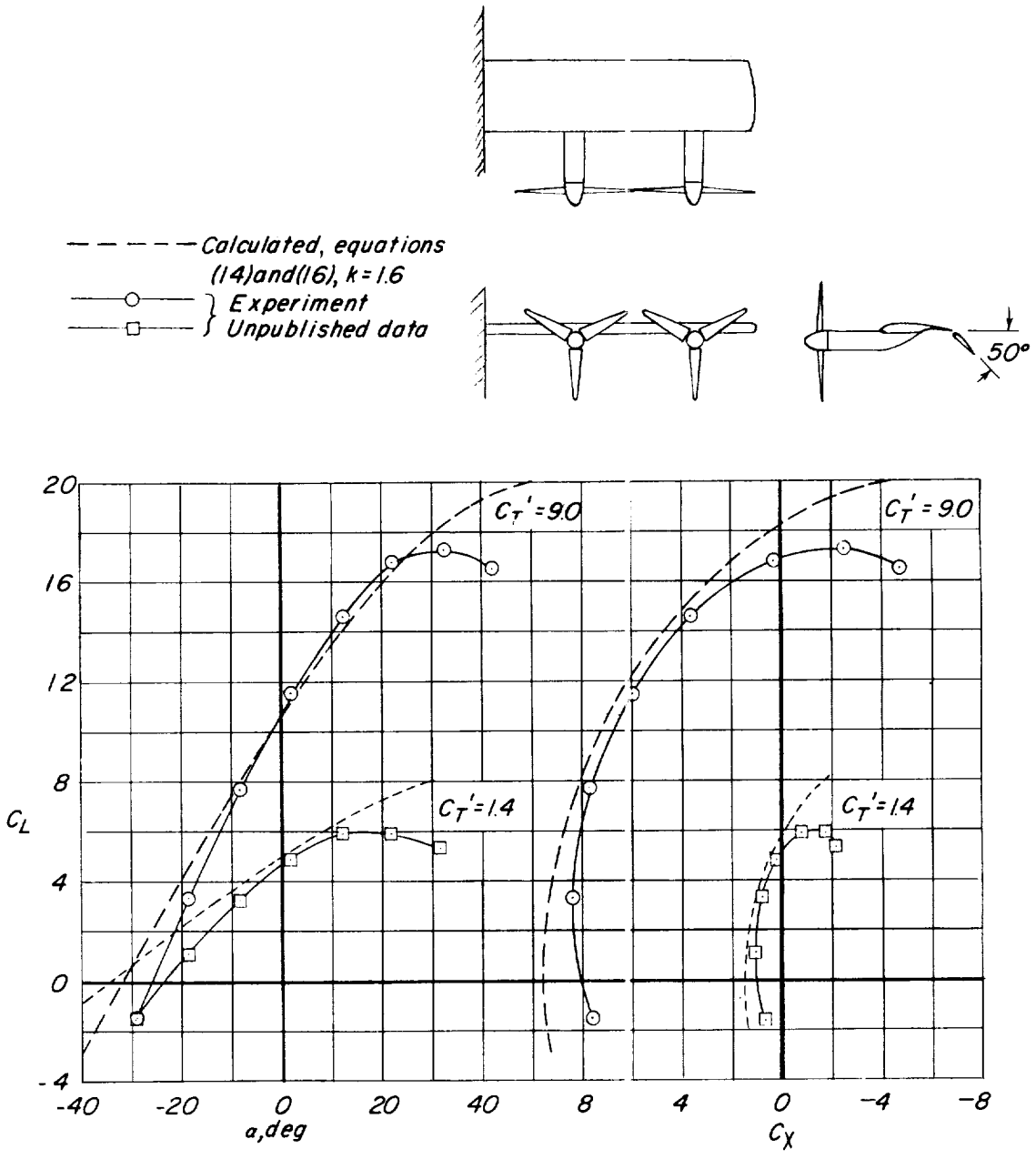

(a) Sliding flap retracted; Fowler flap, $\delta = 50^{\circ}$.

Figure 8.- Comparison of calculated and experimental data for model of reference 10.

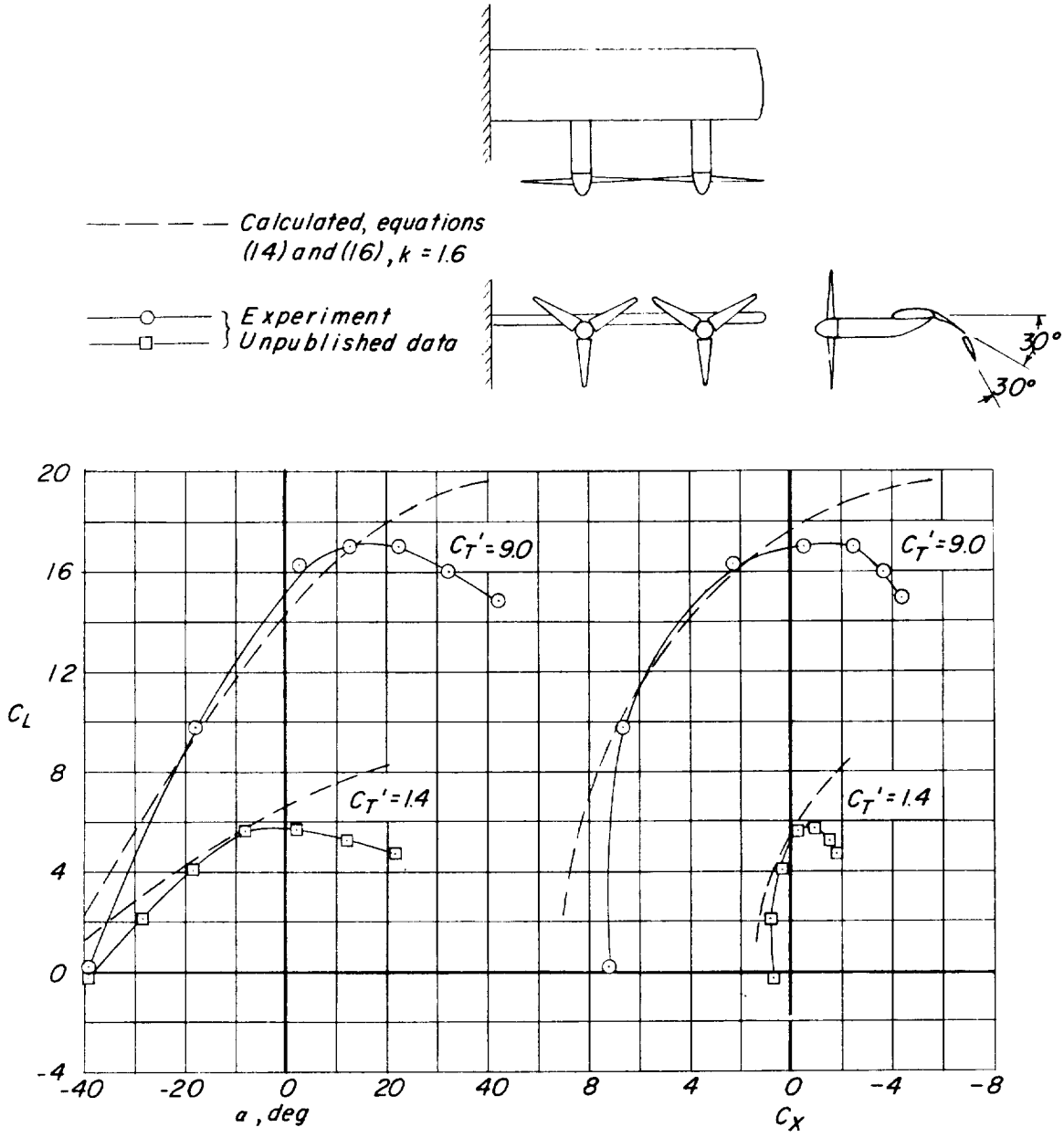

(b) Sliding flap, $\delta = 30^\circ$; Fowler flap, $\delta = 30^\circ$.

Figure 8.- Continued.

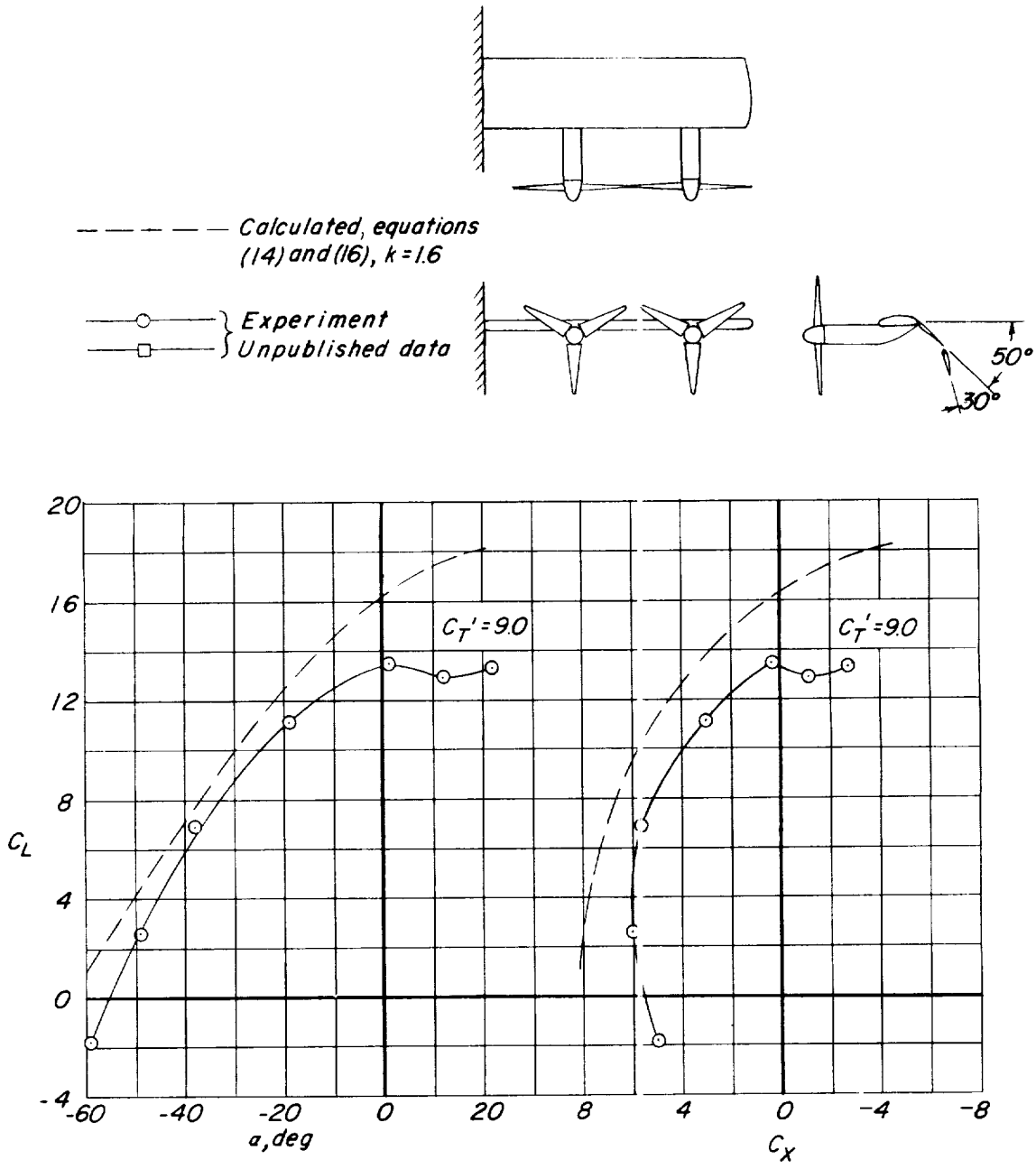

(c) Sliding flap, $\delta = 50^\circ$; Fowler flap, $\delta = 30^\circ$.

Figure 8.- Concluded.